JOURNAL OF MATERIALS SCIENCE **36** (2001) 5853–5860

Quasi-static and dynamic crushing of empty and foam-filled tubes

I. W. HALL*, O. EBIL‡
*Departments of *Mechanical Engineering, ‡Materials Science and Engineering, University of Delaware, Newark, DE 19716, USA*
E-mail: hall@me.udel.edu

M. GUDEN
Department of Mechanical Engineering, Izmir Institute of Technology, Izmir, Turkey

C.-J. YU
Fraunhofer Center-DE, Newark, DE 19711, USA

Metallic foam-filled tubes and their empty counterparts have been tested at quasi-static and dynamic strain rates in order to determine their energy absorption capabilities. Data from the Split-Hopkinson Pressure Bar have been used to generate force vs. displacement curves that are somewhat analogous to pseudo-engineering stress-strain curves. Force balance calculations have also been made. These results indicate that, on an equal weight basis, foam-filled tubes offer greater energy absorption capability than empty tubes at quasi-static strain rates. However, the benefit of foam filling does not appear to be extended to strain rates of the order of 200–500 s^{-1}. Force balance calculations are shown to have potential as a method for monitoring the crushing of metallic foams at high strain rate.

1. Introduction

Metallic foams are materials of increasing importance because they may have good energy absorption capabilities, as well as other properties such as damping, insulation, specific stiffness and fire retardant properties. The emerging body of literature details a variety of methods of foam production via, for example, powder metallurgy or liquid metal routes. Also, a fairly detailed understanding of their mechanical properties has been developed, supported by extensive modeling [1]. Although the majority of available data, to date, concerns conventional quasi-static test data, some high strain rate data have also been presented.

One interesting application of metal foams has been as a filling material to improve the stiffness of hollow sections [2, 3], rather analogous to the use of aluminum honeycombs [4]. This may be important where crashworthiness is a major concern, and knowledge of their dynamic properties would clearly be critical. There is already evidence that filling aluminum or steel tubes with aluminum foam affects the buckling characteristics [3].

The present work was initiated, therefore, to investigate strain rate effects on the deformation behavior and energy absorption capability of simple foam-filled sections. It will be shown that strain rate exerts a significant effect upon these parameters. This report also presents several avenues that have been identified for further exploring the high strain rate deformation of foams and which will be the subjects of future work.

2. Experimental

The Al-1.5%Mn alloy tubes were 7.14 mm in outside diameter with a wall thickness of 0.35 mm. A foamable aluminum alloy containing a small percentage of TiH_2 was prepared by a powder metallurgical process as described by Yu *et al*. [5]. Foam filling was then achieved by inserting small rods of the foamable material into the aluminum tubes and putting them into a furnace to activate the foaming reaction. Precise processing conditions depend to some extent upon the equipment used but, for the specific furnace used here, preliminary experiments established that the optimum foaming temperature for these samples was very close to the melting point of aluminum and the optimum time was 4–4.5 minutes. Foam-filled samples with different length/diameter (l/d) ratios between 1 and 5 were prepared and tested. In order to compare tubes in the same heat treated condition but with and without foam-filling, a set of empty tubes were also tested after being subjected to a similarly extreme heat treatment of 4 min. at 635°C. Finally, another set of empty tubes was tested in the as-received (AR) condition with no further heat treatment. Thus, three sets of samples were tested, referred to as (i) filled (ii) heat treated and (iii) AR (empty but not heat treated).

High strain rate tests (10^2–10^3 s^{-1}) were performed using a Split Hopkinson Pressure Bar (SHPB) apparatus [6, 7] equipped with aluminum bars 3.53 m long and 19 mm in diameter. The samples are compressed by accelerating the striker bar from a gas chamber so that

it impacts the incident bar. The resulting elastic wave travels down the incident bar to the specimen/bar interface where part of the wave is reflected and part continues through the sample and into the transmitter bar. The incident, transmitted and reflected waves are measured by strain gages on the bars. Among other factors, strain rate depends on the speed of striker bar generating the elastic wave, and this is controlled by adjusting the pressure in the chamber. Calibration experiments were performed and two different chamber pressures were then used for each l/d ratio to produce nominal initial strain rates of the order of $\sim 200 \pm 25$ s^{-1} and $\sim 500 \pm 45$ s^{-1}. The elastic wave speed in the aluminum bars was 5064 m s^{-1}.

High strain rate testing of foams with the SHPB is exceptionally problematical. One major reason is that the transmitted wave signals generally exhibit a low signal to noise ratio (this has prompted the use of viscoelastic polymeric materials for the bars [8, 9]) but most importantly because, among other assumptions, the standard treatment of SHPB data to permit the extraction of stress/strain curves assumes a homogeneous stress state and that the sample is of constant volume. These conditions are clearly violated when testing foams, in particular because their collapse is progressive and completely inhomogeneous. Consequently, it must be borne in mind that conventional data reduction routines for generating stress strain curves of fully-dense materials [7, 10] should be viewed with extreme caution. Nevertheless, as a first approximation, and in the absence of any more satisfactory current approach, force vs. displacement curves were generated for each sample as an aid to interpreting the observations. The conventional equations for strain and stress are used, namely:

$$\varepsilon = \frac{-2C_b}{L_s} \int_0^t \varepsilon_r \, dt \tag{1}$$

$$\sigma = \frac{A_b}{A_s} E_b \varepsilon_t \tag{2}$$

Subscripts r and t (and, later, i) refer to reflected, transmitted (and incident) waves, C_b is the elastic wave velocity in the bar, and A_b and A_s are the cross-sectional areas of the bar and sample respectively, and L_s is the sample length. The displacement and force on the sample can be determined by omitting L_s and A_s from the respective equations.

"Pseudo-engineering stress/engineering strain" curves could be generated by dividing by the cross-sectional area and sample length respectively according to Equations 1 and 2, however, uncertainty in determining the actual load-bearing area of the foam makes force/displacement curves more meaningful comparators.

Several reflections of the waves occur during a test and, since (a) no momentum trap was used and (b) the sample remained in place between the bars for several wave reflections, the total strain was accumulated in several successive loading events. Also, it should be noted that no dispersion or other corrections have been applied and, consequently, many of the curves show the well-known Pochhammer-Chree oscillations [11] at low strains. However, the effects discussed below are not fine-scale or subtle and would not be significantly altered by the use of correction routines even if there were any available for foams.

Since the deformation modes strongly depend on the sample geometry, alignment of the sample prior to testing is a major concern. Sample ends were prepared in a precision jig to ensure that, before testing, the faces were perfectly flat and parallel to each other as well as perfectly perpendicular to the compression axis. Despite the attention paid to this aspect, material inhomogeneities in the tube and foam led inevitably to macroscopic buckling of the longer tubes after relatively small strains. During the early stages of deformation, the longer samples ($l/d = 5$, with a length of $\sim$35 mm) resembled samples with $l/d = 1$ or 2, but soon afterwards they underwent gross macroscopic buckling. For this reason, the majority of the data presented below concerns just the first two wave passages.

Force balance calculations were carried out by first time-shifting the incident, reflected and transmitted waves to begin at the same point, and calculating the force due to each wave. Then the total force resulting on the incident bar/sample interface of the sample can be calculated as $(F_i + F_r)$ where F_i is compressive and F_r is tensile. Similarly, the force on the sample/transmitter bar interface is calculated from F_t. A more rigorous version of this approach, incorporating a higher sampling rate and dispersion correction, was used by Li and Lambros [12] to investigate stress homogenization in fiber reinforced composite samples. If the sample is in a state of homogeneous stress, we expect that:

$$(F_i + F_r) = F_t \tag{3}$$

Quasi-static tests were performed to strains of $\sim$70% on a screw-driven Instron machine at a crosshead speed of 2×10^{-3} mm s^{-1}. Thus, in summary, tests were performed at three strain rates, on samples of three different l/d ratios, and on samples of three different types (filled, heat treated and AR), using at least three replicate samples each time.

3. Results

Before presenting the data it should be mentioned that, although the following figures are illustrations of individual tests, there was some variability between nominally identical tests. This arose because of local variations in foam density which were unavoidable with the small samples used. Nevertheless, the variability could be almost entirely removed by normalizing by the sample weight. When plotted on this basis, the experimental curves superimposed well, indicating excellent reproducibility and also demonstrating the strong effect of foam density on individual test results. This illustrates the desirability of reporting the measured density for metallic foams.

3.1. Force vs. displacement

3.1.1. Quasi-static testing

Quasi-static data are presented first as a convenient baseline. Fig. 1 shows compressive force/displacement curves for all three types of samples with a $l/d = 2$. It is noted that the AR and heat treated samples show

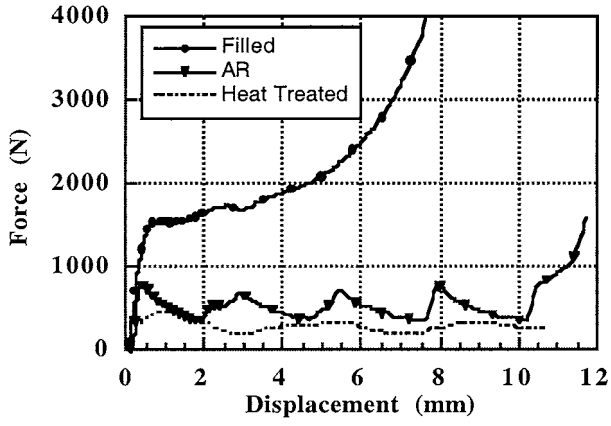

Figure 1 Quasi-static compression test data for foam filled, AR and heat treated samples.

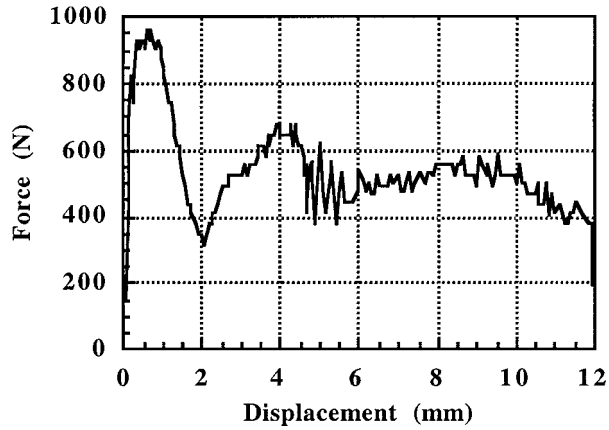

Figure 3 Force vs. displacement curve for an AR tube, $l/d = 2$, tested at $\sim 500\ s^{-1}$.

clearly serrated flow curves where each serration was observed to correspond to the nucleation of a new fold in the tube wall: heat treated tubes, however, show less frequent folding than AR tubes. Although it is clear that the heat treated tube has a considerably reduced flow curve when compared with the AR tube, the flow curve for the filled tube nevertheless lies well above both of them. Thus, despite the high temperature treatment that accompanies the foaming process and greatly softens the tube itself, foam filling produces a very significant strengthening effect. Folding also occurred in the filled tubes but was not accompanied by clear serrations in the force/displacement curves.

The parameters actually measured during testing, i.e. force and displacement, allow the work done in deforming the samples to be calculated. This was evaluated at 1 mm displacement increments and then normalized for each type of sample on the basis of the sample weight. The results are presented in Fig. 2. and show a clear increase in specific work for the foam filled sample. It appears, therefore, that foam filling presents clear advantages in terms of energy absorption, even on an equivalent weight basis, and that the advantages become greater as the total displacements (or strains) increase.

3.1.2. High strain rate testing

Fig. 3 shows the force vs. displacement curve generated by the passage of two compressive waves through an AR sample, $l/d = 2$, tested at a strain rate of approximately $500\ s^{-1}$. The corresponding impact velocity of the bar is $\sim 7\ m\ s^{-1}$. It is seen that the initial peak load is followed by a severe load drop and successive oscillations corresponding to fold generation. The onset of the second wave is marked in this and subsequent figures by the reoccurrence of the Pochhammer-Chree oscillations, in this instance at a displacement of ~ 5 mm. The load maxima appear at approximately the same displacements as for quasi-static tests.

Fig. 4 shows data for a filled sample, $l/d = 2$, also tested at approximately $500\ s^{-1}$. The rapid Pochhammer-Chree oscillations are again seen at the onset of each wave in these samples but there is no indication of the occurrence of folds. Again this is analogous to the behavior of the filled sample shown in Fig. 1. The rapidly rising force at higher displacements shows the typical effect of densification of the foam. The lower plateau stress in Fig. 4 in comparison with Fig. 1 is further evidence of the importance of taking density into account and is not believed to indicate a strain-rate effect.

Comparing Figs 3 and 4, it is seen that at displacements between ~ 4 mm and ~ 10 mm, the increase in force due to the presence of foam is on the order of a factor of ~ 2.5, although this would be expected to increase as the foam densifies. When compared with Fig. 1, the corresponding factors at quasi-static strain rate were between 3 and 9.

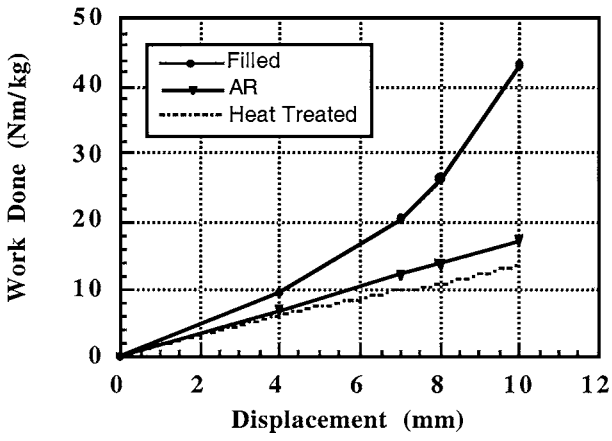

Figure 2 Work done (normalized by total sample weight) as a function of displacement during compression.

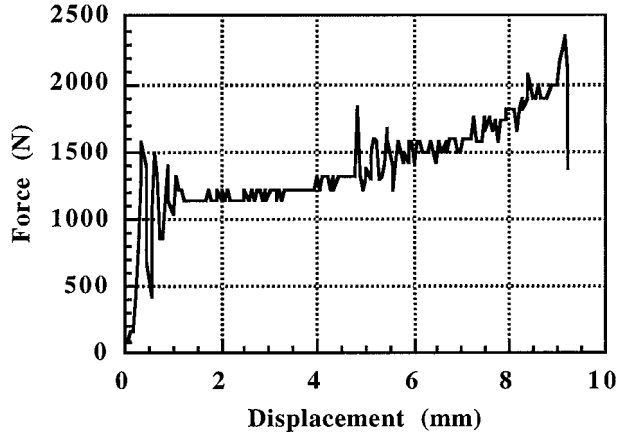

Figure 4 Force vs. displacement curve for a foam filled sample, $l/d = 2$, tested at $\sim 500\ s^{-1}$.

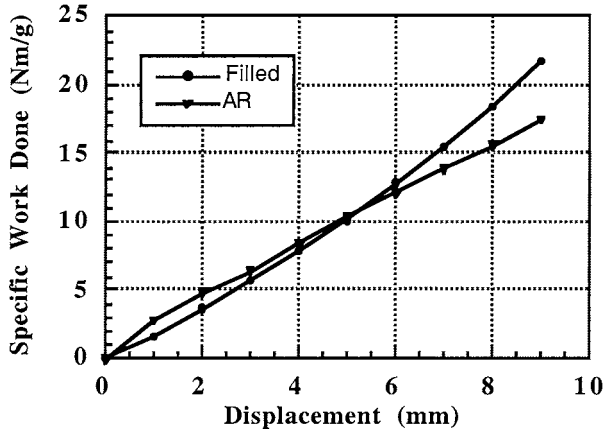

Figure 5 Work done (normalized by total sample weight) as a function of displacement during compression: $l/d = 2$, ~500 s^{-1}.

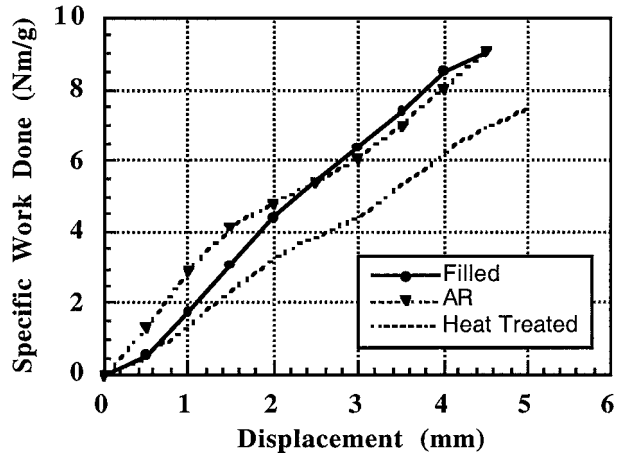

Figure 7 Work done (normalized by total sample weight) as a function of displacement during compression: $l/d = 2$, ~200 s^{-1}.

Next, as for the quasi-static data, specific work vs. displacement curves were generated. Fig. 5 shows the data for AR and filled tubes only and shows that, on an equivalent weight basis, the work done in deforming the tubes is essentially the same up to displacements of ~6 mm irrespective of whether they are foam-filled or not. At higher deformations, the advantages of the foam filled tube again begin to be noted.

Data for a series of samples tested at a lower strain rate (~200 s^{-1}) are shown in Fig. 6 comparing filled, empty and AR tubes. During these tests, the total strain that accumulates during passage of the first two waves is substantially smaller because of the lower striker bar velocity but the same major features can be observed. Again, very marked drops are seen in the force vs. displacement curves when folds occur in the heat treated and AR tubes. Foam-filled tubes on the other hand do not exhibit such pronounced drops and also show substantial hardening between successive peaks. The Pochhammer-Chree oscillations are again shown most clearly by the filled tubes.

Fig. 7 shows the cumulative work done in compressing the sample a total of >4 mm and is calculated using the data of Fig. 6, normalized as before by the sample weight. Again, no advantage accrues through use of the foam within the small displacements investigated, although its advantages would be expected to appear at higher displacements.

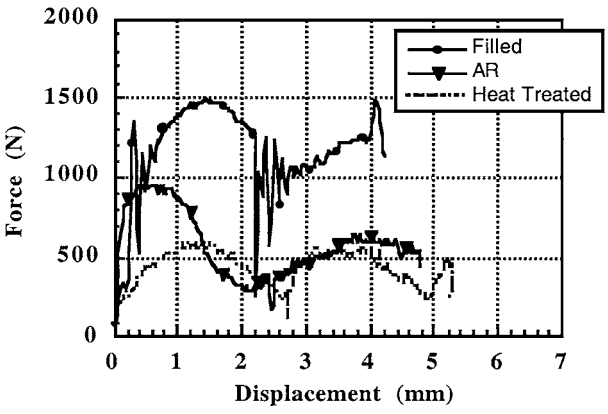

Figure 6 Compression test data for each type of sample showing passage of first two waves, $l/d = 2$, ~200 s^{-1}.

Tests performed with samples of the three different aspect ratios are compared in Fig. 8a and b, which show the force vs. displacement curves for AR and filled samples respectively tested at a strain rate of approximately 200 s^{-1}. Normalizing the data for foam-filled tubes on the basis of total sample weight again leads to substantially similar initial force maxima: thereafter, folds begin to appear for samples with $l/d = 1$ and 2, while the $l/d = 5$ sample does not exhibit its first folding event within the range of displacements examined here.

Experiments were performed in which many reflections of the waves were recorded. The raw data from such an experiment on a filled tube, $l/d = 2$, are presented in Fig. 9. The figure shows that the magnitudes of the incident and reflected waves diminish and that of the transmitted wave increases with each successive passage until, after the passage of ~7 waves, the magnitudes of each are similar. The cumulative force displacement curve for this sample is shown in Fig. 10. In reducing these data, no attempts were made to account for dispersion or attenuation in the bar. Thus, for second and subsequent waves, the reflected (tensile) wave in the transmitter bar was simply subtracted from the following compressive wave in the transmitter bar to determine the total force on the sample according to Equation 2.

3.2. Force balance

As outlined above, data reduction from SHPB experiments allows the calculation of the forces at the front and rear faces of the sample at the same moment in time. Ravichandran and Subhash [13] showed that, for a ceramic sample, a homogeneous stress-state exists after ~4 reflections of the wave within the sample: when this situation applies, the forces at the front and back faces should be identical.

The results of force balance calculations for the passage of the first wave are shown in Fig. 11a and b for examples of AR and foam filled samples respectively, both with $l/d = 2$ and tested at ~500 s^{-1}. The data are presented simply as voltages measured from the strain gages on the bars, and scale directly with the corresponding forces. For the empty tube it is seen that the amplitude of the transmitted wave signal closely

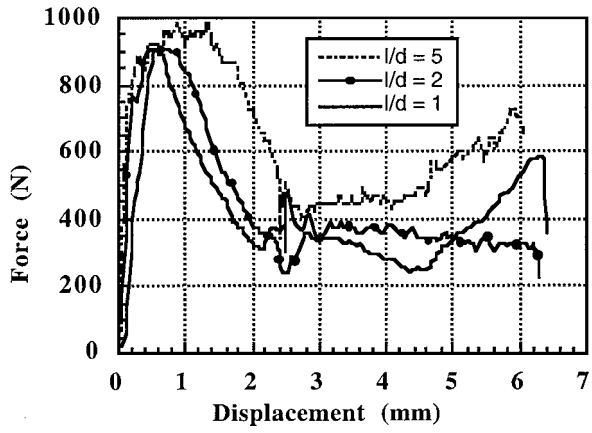

(a)

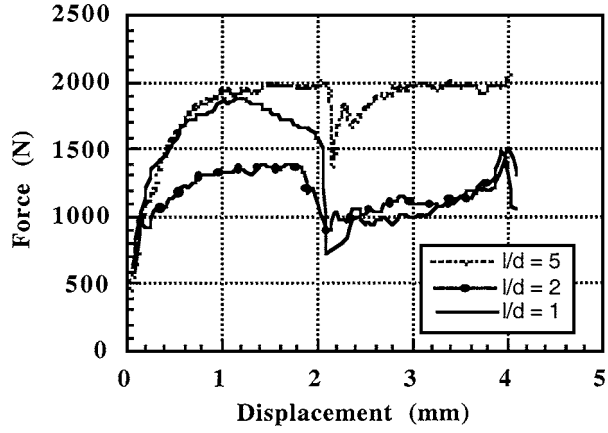

(b)

Figure 8 (a) Compression test data for AR tubes of each l/d ratio at $\sim$200 s^{-1}. (b) Compression test data for foam-filled tubes of each l/d ratio at $\sim$200 s^{-1}.

corresponds to the amplitude of the incident plus reflected wave signal, particularly after the first few microseconds of the test. The stress homogenization time for an Al sample of these dimensions would be approximately 10 μs [13]. The 'noise' in the incident-reflected wave signal arises due to the subtraction of two large numbers each with a small amount of uncertainty.

However, for the filled tube, Fig. 11b, there is a definite discrepancy between the two curves. At times less than $\sim$200 μs, the compressive stress on the front surface is somewhat greater than that at the rear face but at times greater than $\sim$300 μs it reaches levels that are twice that at the rear face. This clearly indicates that conditions of stress homogeneity are not remotely achieved during the test, and possible reasons for this are discussed further below.

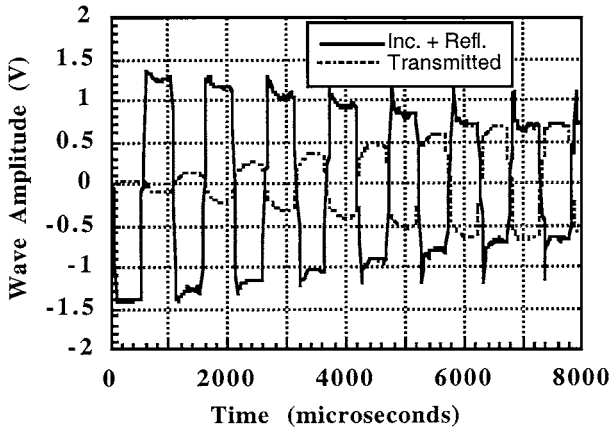

Figure 9 SHPB output data (strain gage voltage vs. time) showing passage of multiple waves and their attenuation.

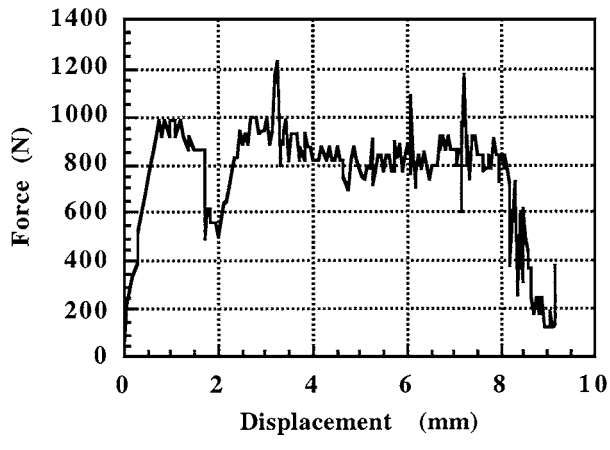

Figure 10 Force vs. displacement curve calculated from data of Fig. 9.

3.3. Observations

Although space limitations preclude an exhaustive description of the deformation modes of all samples, it is nevertheless appropriate to include here several general observations concerning these modes. First, as the tubes deform they undergo consecutive folding events that are plainly reflected in the force/displacement curves. Whereas empty or AR tubes tended to undergo folding at only one end, Fig. 12a, in filled tubes the folds tended to be widely separated. For example, they tended to undergo folding at one end first, then at the other and then in the middle, Fig. 12b, as illustrated also by Seitzberger *et al.* [2] for aluminum filled steel tubes.

In many instances, non-axisymmetric deformation occurred, particularly for the longer tubes and at higher strains. This was due to a combination of the somewhat variable foam structure, illustrated as Fig. 13, along with slight geometrical or property inhomogeneities induced by the foam filling or heat treatment processes which, it must be realized, are rather severe.

4. Discussion

Considering first the quasi-static data, Fig. 1 clearly shows that foam-filling significantly increases the force necessary to deform the tubes. Even when this is normalized with respect to weight, Fig. 2, the foam-filled tubes give an approximately two-fold improvement in energy absorption even at small strains and this advantage becomes even greater as densification of the foam takes place at higher strains. Han *et al.* [14] have shown that Al foams exhibit a peak in energy absorbing capacity at strains of 0.15–0.35; present results show a steadily increasing efficiency of energy absorption due, presumably, to a coupling effect between the tubes and foam. The improvement in energy absorption capacity is considerably greater than the 40–60% found by Seitzberger *et al.* [2], due largely to their use of steel tubes rather than aluminum.

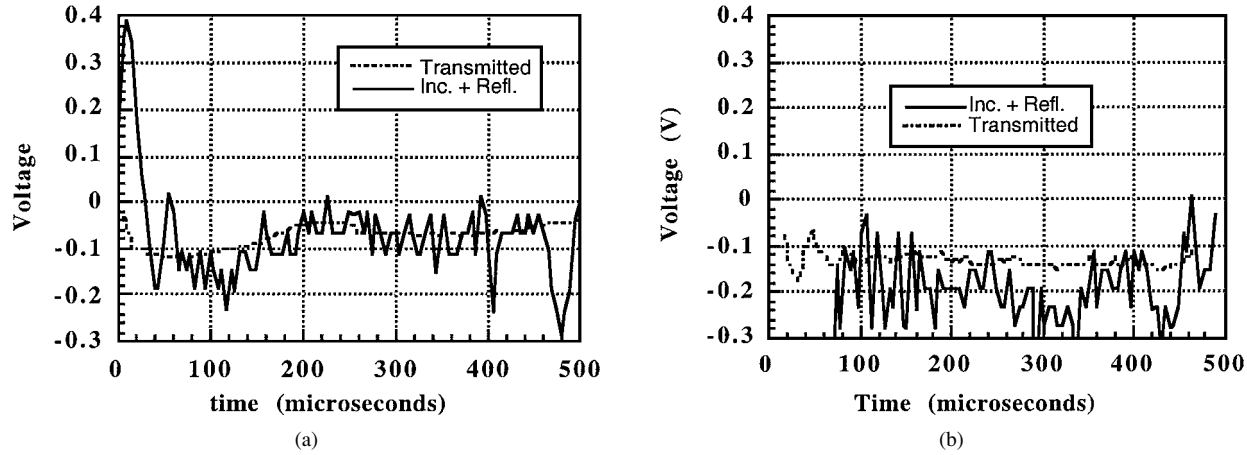

Figure 11 (a) Plot of (incident plus reflected) wave voltage vs. time and transmitted wave voltage vs. time for an AR sample: $l/d = 2$, at $\sim 500\ s^{-1}$. (b) Plot of (incident plus reflected) wave voltage vs. time and transmitted wave voltage vs. time for a foam filled sample: $l/d = 2$, at $\sim 500\ s^{-1}$.

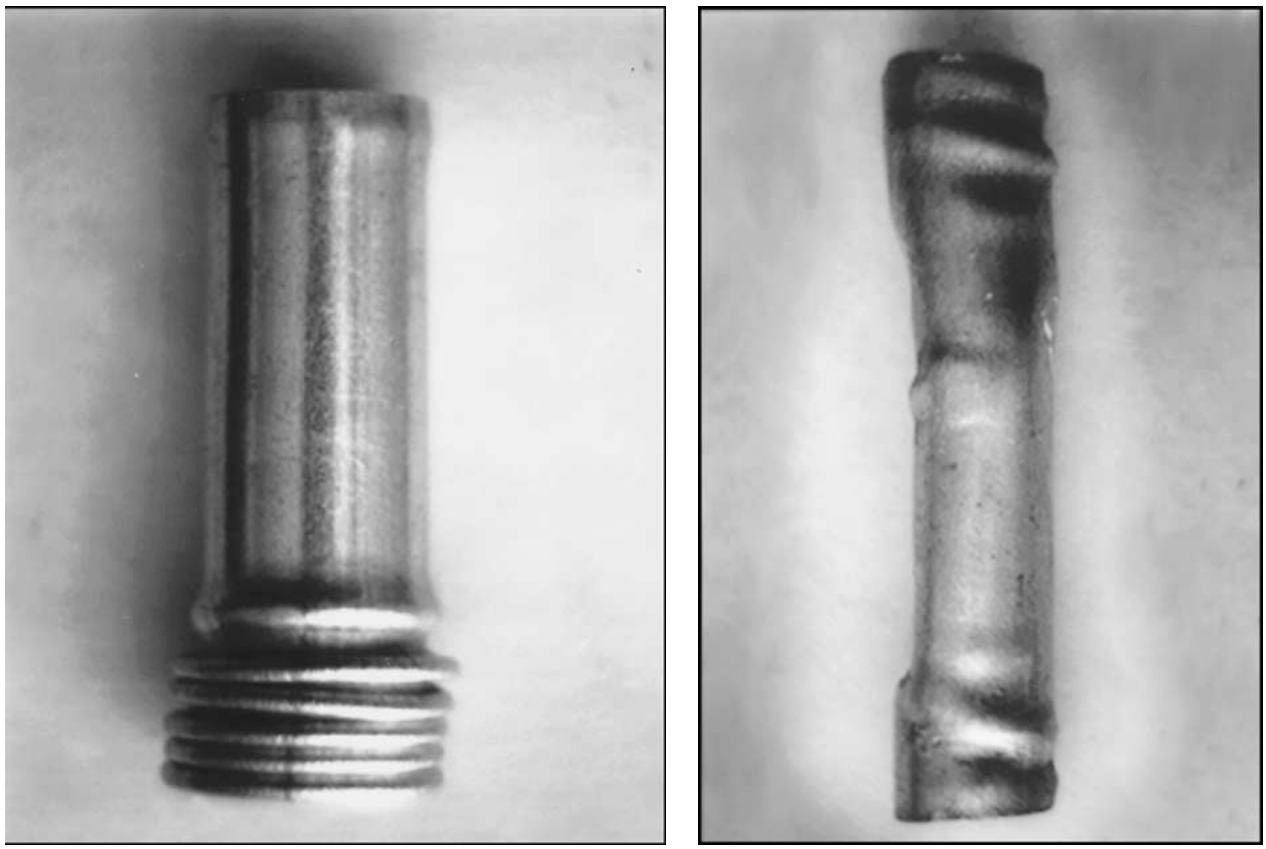

Figure 12 (a) AR sample, tested at 500 s^{-1}, $l/d = 5$, showing folding from one end only. (b) Filled sample, $l/d = 5$, tested at 500 s^{-1}, showing folding at both ends and in central section.

However, when the analogous tests were performed at high strain rates, the situation appeared rather different. Although foam filling still produced a significant increase in the force necessary to impose an equivalent total deformation (compare Figs 3 and 4), this did not translate unambiguously into an advantage in terms of the work (or energy) of deformation on a weight basis. Figs 5 and 7 show that the specific work is essentially identical for AR and foam filled tubes up to displacements of $\sim$6 mm. In other words, the advantage that the foam conferred at quasi-static strain rates did not apparently carry over to higher strain rates in this geometry for the limited displacements tested here.

The principal reason for this apparent discrepancy may lie in the force balance calculations. These indicate, as expected and within the accuracy of the present experiments, that deformation of AR tubes is relatively homogeneous after some tens of microseconds, Fig. 11a, while by contrast, and also as anticipated, deformation of foam-filled tubes is highly inhomogeneous, Fig. 11b. Specifically, the data show that the force at the entry surface of the sample is greater than at the exit surface. The forces used in preparing Figs 5 and 7 were calculated at the rear face of the sample from Equation 2. Entirely different results are produced by using the forces calculated from the front face and,

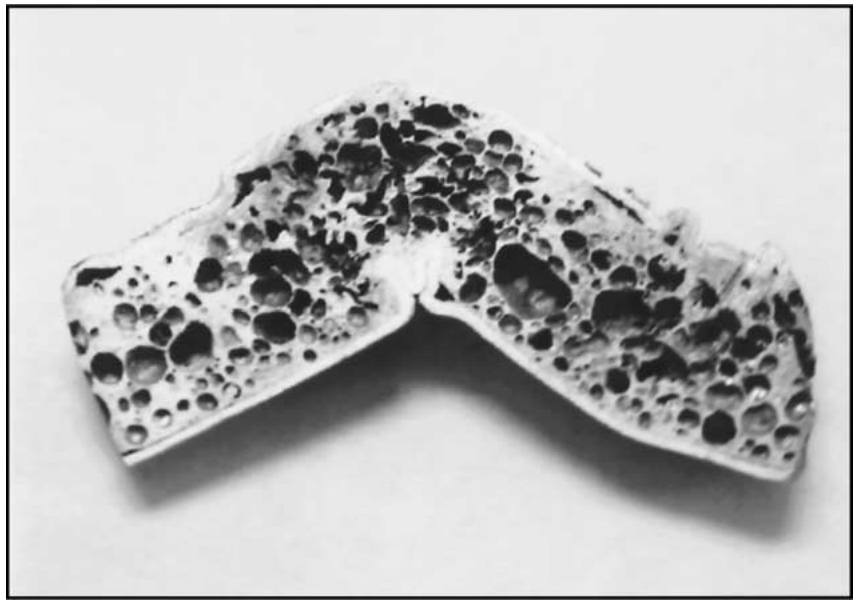

Figure 13 Section through a filled tube ($l/d = 5$, 200 s^{-1}) after severe folding, showing crush zone adjacent to the major fold and variable pore size.

since the forces there are greater, comparison between filled and AR tubes would give a much more favorable edge to the filled tubes. Hence, the front face calculations give an overly optimistic estimate and rear face calculations give an overly pessimistic measure of the work of deformation.

While Fig. 11a and b presents an appearance that might be associated with plastic shock wave effects, calculations from the treatment in [1] show the plastic wave speed in the densified layer of foam to be $\sim$190 m s^{-1}. Since, as mentioned above, the striker bar speed is only $\sim$7 m s^{-1} plastic shock can be eliminated. The situation is actually complex and is currently the subject of further study and modeling but briefly, it is envisaged that several processes occur. After $\sim$10 μs, 3–4 *elastic* wave reflections have occurred in the tube and foam ($l/d = 2$) and stress equilibrium has been temporarily achieved. However, progressive plastic deformation of the foam then occurs leading to a prolonged period in which the sample impedance changes constantly and the stress becomes increasingly inhomogeneous. Finally, after $\sim$320 μs, $\sim$3–4 *plastic* wave reflections have occurred and a homogeneous stress state is re-established: Fig. 11b actually shows this to occur after $\sim$350 μs, well within the present limits of experimental accuracy.

The question then becomes "how to make a reasonable and realistic determination of energy absorption (or even just the stress/strain curve) at high strain rates?". The present results show clearly that the conventional 1-, 2- or 3-wave treatments [10] are unsatisfactory even if a Plexiglas^{TM} (polymethylmethacrylate) transmitter bar is used to increase the amplitude of the signal [15]. While this is clearly still a subject for considerable further research, the use of the force balance approach would seem to provide a method of studying the process of stress homogenization within the sample since it yields a picture of the forces at each face simultaneously. Monitoring the change in these stresses as a function of increasing strain can provide a tool for monitoring the densification process. Further work is under way to see how the force balance changes at higher displacements and to determine whether it is indeed possible to track densification of the sample using these measurements. These results will be presented elsewhere.

Tests to investigate the effect of aspect ratio showed that, for AR tubes, the forces at which at least the first two folds occur are reasonably consistent and are independent of sample length. However, the forces at which they occur, $\sim$1000 N and 1200 N, were somewhat higher than was the case for quasistatic tubes where the folds occurred at $\sim$800 N. Since aluminum alloys exhibit only very weak strain rate dependence over the present strain rate range [16], this indicates a degree of strain rate sensitivity of the buckling stress. The corresponding picture for filled tubes, Fig. 8b, is less clear insofar as the curves show a little more variability: only some of this variability can be removed by normalizing with respect to sample weight as before. Nevertheless, if one selects a specific displacement, e.g. 2 mm, it is found that the average force necessary to cause this displacement in the filled tube is 1500–1600 N at both high and quasi-static strain rates. Thus, first indications are that there is no clear effect of strain rate upon the force necessary to produce buckling or equivalent deformations in foam filled tubes. Mukai *et al.* [17], however, found that a closed cell aluminum foam exhibited remarkable strain rate sensitivity, although their results concerned higher strain rates of 2.5×10^3 s^{-1} and this is within the strain rate range where Al is known to show much increased strain rate sensitivity anyway. Further work is presently underway to clarify this issue.

Finally, it has been demonstrated that force displacement records up to large deformations can be achieved in metallic foams with the SHPB by means of recording several wave reflections as long as the duration of the input pulse and the lengths of the bars permit separation of the waves. Zhao and Gary [18] have used a similar approach, but using a separation of waves technique, to extend the usual strain range available in the SHPB, typically $\sim$20%, to the much higher strains necessary for investigation of polymeric foams.

5. Conclusions

Tests have been conducted at quasi-static and dynamic strain rates on empty, heat treated, and foam filled aluminum tubes. On an equal weight basis, foam filled tubes absorb significantly more energy than empty tubes at quasi-static strain rates. For small strains at high strain rates, the corresponding advantages of foam filling have not yet been clearly demonstrated. Nevertheless, based upon calculation of forces on the back faces of samples, it is likely that the advantages become more important at higher strains. The inhomogeneity of plastic deformation of metal foams is evidenced by the imbalance of forces at the sample front and rear faces: this effect may have use as a method of tracking and analyzing the process of foam collapse at high strain rates. A strain rate sensitivity of the buckling stress has been demonstrated for AR aluminum tubes.

Acknowledgments

The authors gratefully acknowledge financial support for this work by Honda R.&D., Americas, Inc., through the award of a Honda Initiation Grant. Thanks are also extended to Prof. J. Lambros for helpful discussions.

References

1. M. F. ASHBY, A. G. EVANS, N. A. FLECK, L. J. GIBSON, J. W. HUTCHINSON and H. N. G. WADLEY, "Metal Foams: A Design Guide" (Butterworth-Heinemann, Woburn, MA 2000).
2. M. SEITZBURGER, F. G. RAMMERSTORFER, H. P. DEGISCHER and R. GRADINGER, *Acta Mechanica* **125** (1997) 93.
3. S. SANTOSA and T. WIERZBICKI, *Comp. and Struct.* **68** (1998) 343.
4. H. ZHAO and G. GARY, *Int. J. Impact. Eng.* **21** (1998) 827.
5. C. YU, H. EIFERT, J. BANHART and J. BAUMEISTER, *Journal of Mat. Res. Innovat.* **2** (1998) 181.
6. U. S. LINDHOLM, *J. Mech. Phys. Solids* **12** (1964) 317.
7. M. GÜDEN and I. W. HALL, *J. Mater. Sci.* **33** (1998) 3285.
8. H. ZHAO, G. GARY and J. R. KLEPACZKO, *Int. J. Impact. Eng.* **19** (1997) 319.
9. O. SAWAS, S. N. BRAR and R. A. BROCKMAN, *Exp. Mech.* **38** (1998) 204.
10. G. T. GRAY III, in "Methods in Materials Research" (Wiley, New York, NY, 1997).
11. M. A MEYERS, "Dynamic Behavior of Materials" (Wiley, New York, NY, 1994).
12. Z. LI and J. LAMBROS, *Comp. Sci. & Tech.* **59** (1999) 1097.
13. G. RAVICHANDRAN and G. SUBHASH, *J. Amer. Ceram. Soc.* **77** (1994) 263.
14. F. HAN, Z. ZHU and J. GAO, *Met. & Mat. Trans. A* **29A** (1998) 2497.
15. V. S. DESHPANDE and N. A. FLECK, *Int. J. Impact. Eng.* **24** (2000) 277.
16. S. YADAV, D. R. CHICHILI and K. T. RAMESH, *Acta Metall. Mater.* **43** (1995) 4453.
17. T. MUKAI, H. KANAHASHI, T. MIYOSHI, M. MABUCHI, T. G. NIEH and K. HIGASHI, *Scripta Mater.* **40** (1999) 921.
18. H. ZHAO and G. GARY, *J. Mech. Phys. Solids.* **45** (1997) 1185.

Received 28 September 2000
and accepted 3 August 2001